Firstly, we would like to thank both referees for their important comments, and we have revised our manuscript accordingly. The original comments from referees are in black, our replies are in blue and the changes in original manuscript are in red.

Following the two reviewers' comments, we have revised the description of the methods and related discussions. Furthermore, we have included results and discussions to reinforce that localized plumes and nearby human activities had only a minor influence on our findings, and we focused on characterizing the aerosol physicochemical properties within the regionally transported air masses. Our results clearly show that, during daytime, our site was mostly affected by air masses transported from various regions of Europe, containing both anthropogenic and biogenic influences. We could therefore define a photochemical clock based on NO_x/NO_y ratio as the "Relative anthropogenic photochemical age". This metric reflects the extent of photochemical processing of the regionally transported air mass, and it is not directly linked to the diurnal variation of other atmospheric constituents at this forest site. We have revised our abstract and conclusion to clearly summarise our results and to better highlight the key findings of this study. The structure of the manuscript has also been reorganized to address the reviewers' comments.

The Abstract has been revised as:

Organic aerosols (OA) play a significant role in influencing both climate and human health. However, in source–receptor modeling, a large fraction of OA is typically attributed to highly aged, atmospherically processed species collectively referred to as oxygenated organic aerosol (OOA). However, the formation pathways and evolution of OOA as well as their impacts on aerosol optical properties, remain poorly understood. To address this knowledge gap, an experiment was conducted in a suburban site in the Paris region to study the evolution of OOA and their optical properties. Our results show that in regionally transported air masses with mixed biogenic and anthropogenic emissions, the formation of OOA through photochemical processes explains most of the increase in submicron particle mass. Meteorological conditions played a critical role: under dry and strong solar radiation conditions, rapid formation of more-oxidized OOA (MO-OOA) was observed. The production of MO-OOA importantly contributed to the brown carbon (BrC) increase during the daytime, enhancing short-wavelength light absorption by an average of ~35% following ~24 h of photochemical aging. Conversely, under humid, low-radiation conditions, the OA composition shifted toward less-oxidized OOA (LO-OOA). Suppressed photochemistry limited MO-OOA production, resulting in a lower overall OA oxidation state. These findings highlight the role of photochemistry in shaping both the chemical evolution and resultant optical properties of OA, underscoring the need to consider meteorological dynamics when evaluating aerosol–climate interactions in suburban forest environments.

The conclusion has been revised as:

In this paper, we present a study in a suburban forest region of a European megacity in summer to demonstrate the impacts of photochemical processes on aerosol properties in regionally transported air masses containing a mixture of anthropogenic and biogenic emitted compounds. Based on the detailed mass spectra of the HR-AMS, we resolved primary and secondary OA sources via PMF analysis, enabling quantitative tracking of the evolution of OA during photochemical aging. The evolution of individual PMF-derived OA factors was further examined in relation to aerosol optical properties to determine their respective contributions to BrC. Throughout the entire experiment, OA dominated the total submicron aerosol mass. An increase in OA with relative anthropogenic photochemical age was primarily driven by the production of OOA. The production rates of different OOA types varied with meteorological conditions: dry air masses from NE continental regions coincided with strong solar radiation, while SW marine air masses were associated with humid, low-radiation conditions. OOA formed under humid, low-radiation conditions exhibited a lower oxidation state, reflected in reduced average bulk O:C ratios, with LO-OOA accounting for a substantially larger fraction of total OA. By contrast, intense photochemical activity under dry, high-radiation conditions promoted rapid formation of MO-OOA. Although such strong photochemistry depleted primary anthropogenic OA and nitrogen-enriched LO-OOA, this was offset by enhanced production of MO-OOA and subsequent secondary BrC

formation. Consequently, the fraction of total BrC associated with short-wavelength absorption increased with relative anthropogenic photochemical age. This highlights the critical need to incorporate BrC formation mechanisms into models to accurately simulate direct radiative effect (Drugé et al., 2022).

Reviewer #1

In their manuscript "Impacts of summertime photochemical aging on the physicochemical properties of aerosols in a Paris suburban forest region", authors linked OA factors identified from conventional AMS-PMF approach to air mass origins and photochemical activities, and highlighted the amplified BrC absorption observed during the ACROSS project. The study is on a topic of relevance and general interest to the readers of ACP. However, I found the description of the methodology partially insufficient and partially hindered the evaluation of the results. The below comments need to be addressed first before I could comprehensively evaluate Section 3.3 onward. Therefore, I recommend a major revision and am open to review the manuscript again if needed.

We thank the reviewer for the comments, and we have revised the method section accordingly.

1. Line 46-47, "Rapid urbanization and industrial activities had led to high levels of anthropogenic aerosol emissions in developed megacities (Shi et al., 2019)". I am unable to find much information about "anthropogenic aerosol emissions" from your referred paper. Instead, its winter section stated that "PM2.5 and O3 each had similar temporal patterns at the urban and rural sites (Fig. 5), indicating a synoptic-scale meteorological impact" instead of "anthropogenic emissions". Please make sure the reference is correct and relevant, or modify your sentence correspondingly. One megacity (Beijing) is also insufficient to serve the purpose of representing a generalized statement (developed megacities).

Accept. We have revised our related introduction section, and we have added the studies from more megacities:

Urban areas, with their intensive resource use, are major contributors to anthropogenic aerosol emissions globally (Zhang et al., 2020; Papachristopoulou et al., 2022; Franklin et al., 2025). Therefore, characterizing the physicochemical properties of aerosols is crucial for understanding their impact on climate, air quality, and human health, ultimately informing strategies for mitigation and environmental protection.

2. Line 105: why near-ground measurements (5-m) can "facilitate a focused discussion on regional pollution within the boundary layer" better than the 40-m measurements, if both were available? Aren't the lower measurements more affected by localized plumes or nearby human activities/events? If the PMF results from the below- and above-canopy measurements were consistent to each other throughout the entire campaign, then it could be less of a concern. Otherwise, it is recommended to separate the entire campaign period into episodes with vertical differences in NR-PM1 and those without to discuss separately, as shown in previous AMS-PMF study above- and below-canopy in Michigan, U.S. (Bui et al., 2021). Please clarify.

Firstly, not all the measurements were available for below- and above canopy measurements during the experiment periods; only the HR-AMS was available for measurements at both levels in this study. Secondly, the PMF results showed consistent daytime trends due to well-mixed canopy, whereas opposite trends emerged at night for LO-OOA2, likely linked to monoterpene emissions. This can be attributed to stronger near-ground vegetation emissions when the air masses below- and above-canopy were decoupled at night. Since this study focused on daytime results only, we determined that the influence of localized plumes and human activities near the measurement site during the daytime was minimal and does not compromise our overall findings. However, we still thank the reviewer for the constructive

suggestions; a following separate study focusing on the nighttime differences between above- and below-canopy AMS results during the ACROSS project is in preparation.

We have revised the description in Section 2.1:

In this study, the scope is confined to near-ground measurements as most of the measurement results in this study were only available at the near-ground level.

We have added the discussions about the above- and below- canopy results in Section 3.2:

The comparison between below- and above-canopy PMF results is provided in the Supplementary, showing that the trends of NR-PM_1 and PMF for below- and above-canopy were consistent during the daytime throughout the campaign. Thus, the influence of localized fresh plumes and nearby human activities was minimal since the boundary layer was well mixed during the daytime over the whole the campaign period, supporting our subsequent findings on regional pollution within the boundary layer during the daytime.

We have also included the comparison between below- and above- canopy PMF results and discussions in the supplementary:

Fig. S9 and S10 show the time series of below- and above-canopy NR-PM_1 and diurnal differences in PMF results during the ACROSS project, respectively. Throughout the campaign, differences in NR-PM_1 between the two heights were only observed at night till until the early dawn the next day. This was likely attributed to air masses above- and below-canopy decoupling and near-ground emissions of LO-OOA2 from local vegetation at night. After sunrise (~06:00), the boundary layer height increased, and local emissions became more diluted. Consequently, the above– and below- canopy differences reduced, indicating that the influence of localized emission was minimal during daytime under well-mixed boundary layer conditions.

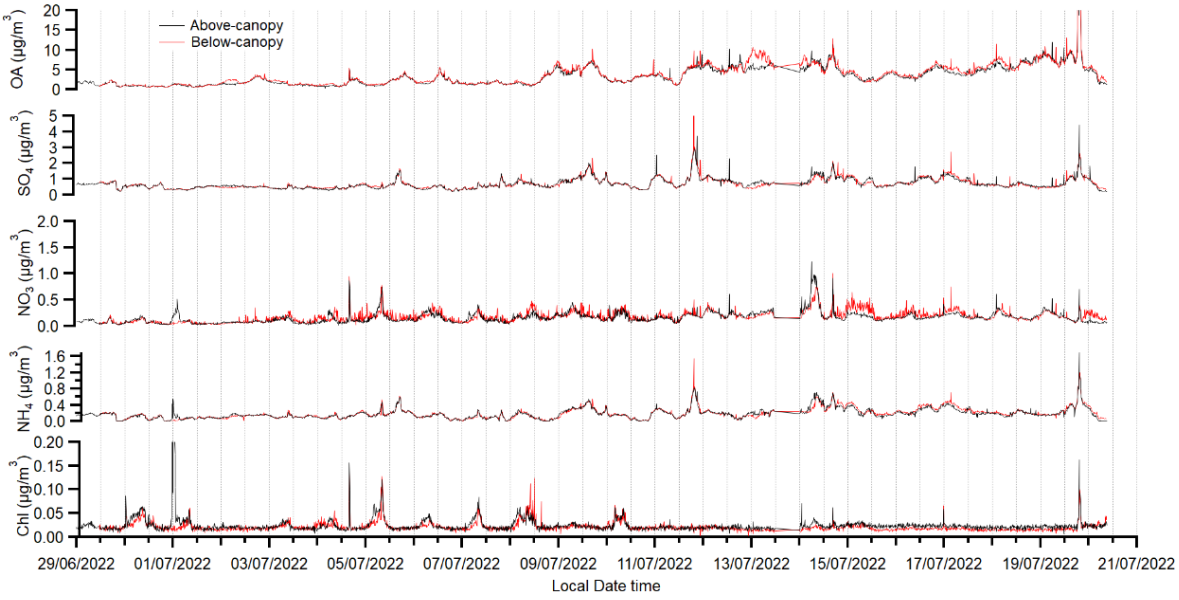

Fig. S9 Time series of HR-AMS NR-PM_1 results below- and above- canopy

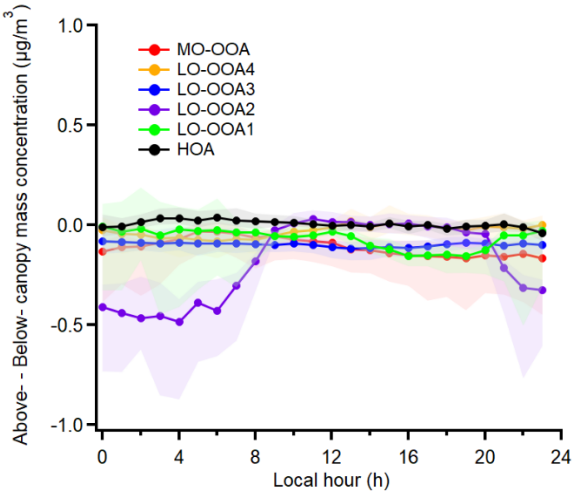

Fig. S10 Diurnal differences in HR-AMS PMF-derived OA factor mass concentrations above and below the canopy. The lower and upper whiskers in the figure are the 25th and 75th percentiles, respectively.

3. More contexts should be provided to Section 2.2:

3.1 HR-AMS section: Middlebrook et al. (2012) should be cited when you mention/use CDCE. How did you treat the RIE for OA since most of your analysis focused on the organics? Did you perform periodical filtered measurement for gas-phase CO2+ subtraction from your sampling and/or calculate species-dependent detection limits?

Thanks for the comments. The standard organic RIE we applied is 1.4. Yes, we performed the periodical filtered daily, and we corrected for gas phase CO2+ subtraction. The RIE information has been included in Table S1 (please refer to our response to comment 3.2). We have revised the related description in our original manuscript:

The Ionization Efficiency (IE) and the Relative Ionization Efficiency (RIE) of the HR-AMS were calibrated using mono-disperse (300 nm), nebulized ammonium nitrate and ammonium sulfate particles, and the IE and RIE results were presented in Table S1. A Composition-Dependent Collection Efficiency (CDCE) was applied to the final results (Middlebrook et al., 2012). Background CO_2 in the HR-AMS was corrected by calibrating the measured CO_2 in filtered air against external measurements obtained with a cavity ringdown spectrometer (CRDS, Picarro G2302).

3.2 HR-AMS section: a table of IE and RIE results, and five main species detection limits should be added to the SI.

Accept. We have added the following table into the supplementary.

Ionization Efficiency (IE)	3.00E-07	
	Relative Ionization Efficiency (RIE)	Detection limit of HR-AMS V-mode (μg/m³)
OA	1.4	0.022
SO4	0.88	0.0052
NO3	1.1	0.0029
NH4	4	0.038
Chl	1.3	0.013

Table S1: Ionization Efficiency (IE) and Relative Ionization Efficiency (RIE) applied for HR-AMS data analysis. The detection limits for each measured compound are from Decarlo et al. (2006).

3.3 HR-AMS section: "all factors exhibited distinct temporal and spectral characteristics until a six factor, and the spectra of the six factors were consistent with source spectra in the AMS spectral database (Jeon et al., 2023)"- please elaborate quantitatively on "distinct" and "consistent" in the SI.

Accept, we have revised the description in Section 2.2.1:

A six-factor solution with fPeak = 0 was chosen as the optimal solution. Although the mass spectra of the OOA factors were highly similar (Pearson correlation coefficient $r > 0.8$), their time series remained distinct, with $r < 0.6$ in the six-factor solution. The spectra of the six factors were comparable to those from previous summer AMS PMF study in Paris urban area (Crippa et al., 2013) documented in the AMS spectral database (Jeon et al., 2023), and the comparison is presented in Table S2 in the supplementary.

We have added the comparison of mass spectra of all the factors with the previous AMS PMF studies in Paris urban area from AMS spectral database, the comparison results is reported as cosine similarity calculated following the methods described by Jeon et al. (2023):

Table S2 presented cosine similarity between the AMS PMF factor mass spectra derived in this study and those from Crippa et al. (2013). Cosine similarity of the AMS PMF factor mass spectra is calculated following the methods described in Jeon et al. (2023). The HOA factor resolved here shows a strong similarity (cosine similarity > 0.9) with the primary OA identified in previous measurements. In Crippa et al. (2013), OOA was further classified by volatility, with Low Volatility (LV)-OOA exhibiting a higher oxidation state than Semi Volatility (SV)-OOA. This classification is consistent with our results: LO-OOA1 and LO-OOA2, characterized by lower O:C ratios, closely resemble the spectra of SV-OOA, whereas LO-OOA3, LO-OOA4, and MO-OOA show stronger similarity with the spectra of LV-OOA.

AMS PMF factors in this study	AMS PMF factors from previous Paris 2009 summer study (Crippa et al., 2013)				
	Cooking OA (COA)	HOA	Semi Volatility (SV)-OOA	Marine OA (MOA)	Low Volatility (LV)-OOA
HOA	**0.91**	**0.92**	0.86	0.76	0.73
LO-OOA1	0.75	0.82	**0.94**	0.86	0.88
LO-OOA2	0.62	0.76	**0.94**	0.88	**0.94**
LO-OOA3	0.41	0.55	0.74	0.76	**0.96**
LO-OOA4	0.38	0.53	0.70	0.76	**0.98**
MO-OOA	0.26	0.39	0.57	0.67	**0.94**

Table S2 Cosine similarity between the AMS PMF factor mass spectra derived in this study and those from previous summer measurements in urban Paris (Crippa et al., 2013). Cosine similarity values greater than 0.9 are highlighted in bold and considered similar.

3.4: AE33 section: from your description, it seems that AE33 was sampling from another platform. Was the AE33 pm2.5-cycloned and Nafion dried as well? How did you treat the different collection efficiencies (line loss) of the two instruments at different platforms using different inlet systems before adding them together for a "total PM1 mass concentration"?

The AE33 was connected to the PM_1 cyclone and Nafion dryer. The two platforms were positioned side by side during the campaign, and we therefore considered that they have comparable sampling efficiency. Although the HR-AMS was operated downstream of a $PM_{2.5}$ cyclone, the aerodynamic lens transmits only submicron particles. Both inlet systems were with very close line loss rates, and loss rates were less than 10% for PM_1 (in maximum, ~4% for the AE33 inlet system and ~6% for the HR-AMS inlet system) following the estimation method described in Von Der Weiden et al. (2009). Therefore, it is reasonable to use the sum of AMS and AE33 results for a total PM_1 mass concentration. The description has been revised as:

The PM_1 aerosol optical absorption coefficient (units of $Mm^{-1} = 10^{-6}$ m^{-1}) at seven different wavelengths (370, 470, 520, 590, 660, and 880 and 950 nm) was measured by a dual-spot aethalometer (AE33, Magee

Sci.) (Drinovec et al., 2015) at the PortablE Gas and Aerosol Sampling UnitS (PEGASUS) mobile platform (Formenti et al., 2025) which was positioned close to the HR-AMS container. The AE33 was operated at a flow rate of 5 L min^{-1} and connected to a PM_1 cyclone and a Nafion drier. The whole inlet system has a total flow rate of around 38 L min^{-1}.

The description about the PM_1 has been revised as:

The total PM_1 mass concentration was determined as the sum of the NR-PM_1 and eBC mass concentration measured by the HR-AMS and the AE-33, respectively. Although the HR-AMS was operated downstream of a $PM_{2.5}$ cyclone, its aerodynamic lens transmits only submicron particles. The two sampling inlet systems showed comparable line loss rates for PM_1, with maximum losses estimated at approximately 6% for PM_1 in both inlet systems following the estimation method described in Von Der Weiden et al. (2009).

3.5: What is your CAPS NO2 instrument model/type?

We have revised the instrument model here:

NO_2 concentration was measured by a chemiluminescence analyzer (HORIBA APNA 370).

3.6: Your net radiometer and wind monitor were mounted on the tower (40-m) while the aerosol instruments were described as near-surface. How did you account for the canopy interference to the solar radiation and wind before they reach the ground level for your subsequent analysis?

We appreciate the reviewer's concern. The measurements were conducted in an open clear area (with a size of 26.5 m × 26.3 m, ~ 697 m^2) within the forest, where canopy interference with solar radiation and wind was minimal. Furthermore, the comparison of HR-AMS results obtained above and below the canopy indicates that the boundary layer was well mixed during the daytime throughout the campaign. Thus, the tower-top observations were representative of the near-surface atmospheric conditions relevant for our metrological measurements.

Combine Reviewer #2's Minor comment 1.2 We have added more description about the site:

A ground-based experiment was conducted in a suburban forest area of Paris (Rambouillet forest) within the framework of the ACROSS project (Cantrell and Michoud, 2022). It was composed of approximately 70% oak, 20% pine, and 10% beech and chestnut trees. The canopy height of the trees in the Rambouillet forest was on the order of ~20 - 25 m. During the campaign, multiple containers were placed side by side in a clear area (with a size of 26.5 m × 26.3 m, ~ 697 m^2) within the Rambouillet forest (48.7 N, 1.7 E) which was ~50 km south-west from the centre of Paris. The broader ACROSS Rambouillet experiment, encompassing both near-ground (~5 m) and above-canopy (on a ~40-m-high tower) measurements, was conducted from June 13th to July 25th, 2022.

We have also revised the description of the meteorological measurements:

The surface downwelling shortwave radiation and wind parameters were measured by a net radiometer (Kipp & Zonen, CNR4: 192119) and a wind monitor (Young, 05103: 4655) mounted on the tower. As the measurements were conducted in a clear area with no trees, the tower-top observations were considered representative of near-surface atmospheric conditions relevant for radiation and wind.

4. Much of the context in Section 3.2 should be put in the SI as an identification & justification of PMF OA-factors instead of as standalone scientific findings. Its corresponding figures are recommended to be combined with figures in Section 3.1 as an overview of campaign measurements (values reporting). For example, I see no reason why Figure 5 (diurnal of OA factors) and Figure 3 (diurnal of other species) are

not combined, and why Figure 4 (TS of OA factors) are not combined into Figure 2 (TS of RH, T, bulk PM species). Having them separately is redundant and makes it harder to see general trends among different parameters.

We thank the reviewer for the comments. Combining both reviewers' comments we have revised Section 3.2. We keep Section 3.2 in the main text as it discusses the potential sources of different PMF-derived OA factors. Following Reviewer 1's comments we have revised part of our figures.

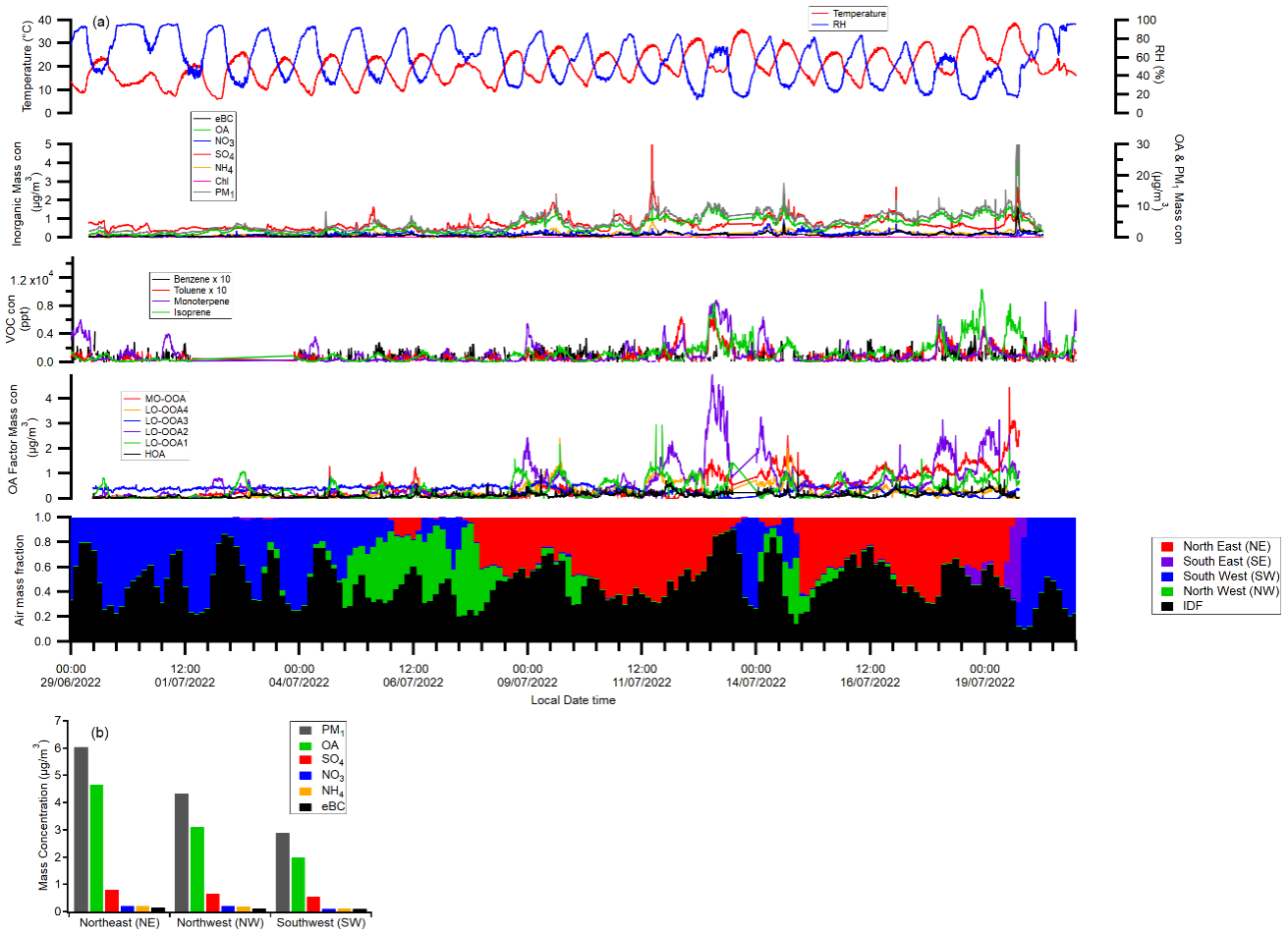

Figure 2: (a) Time series of temperature, RH, PM_1, VOC, PMF-derived OA factors and historic air mass fractions; (b) The average PM_1 composition mass concentrations under different external air mass dominated periods.

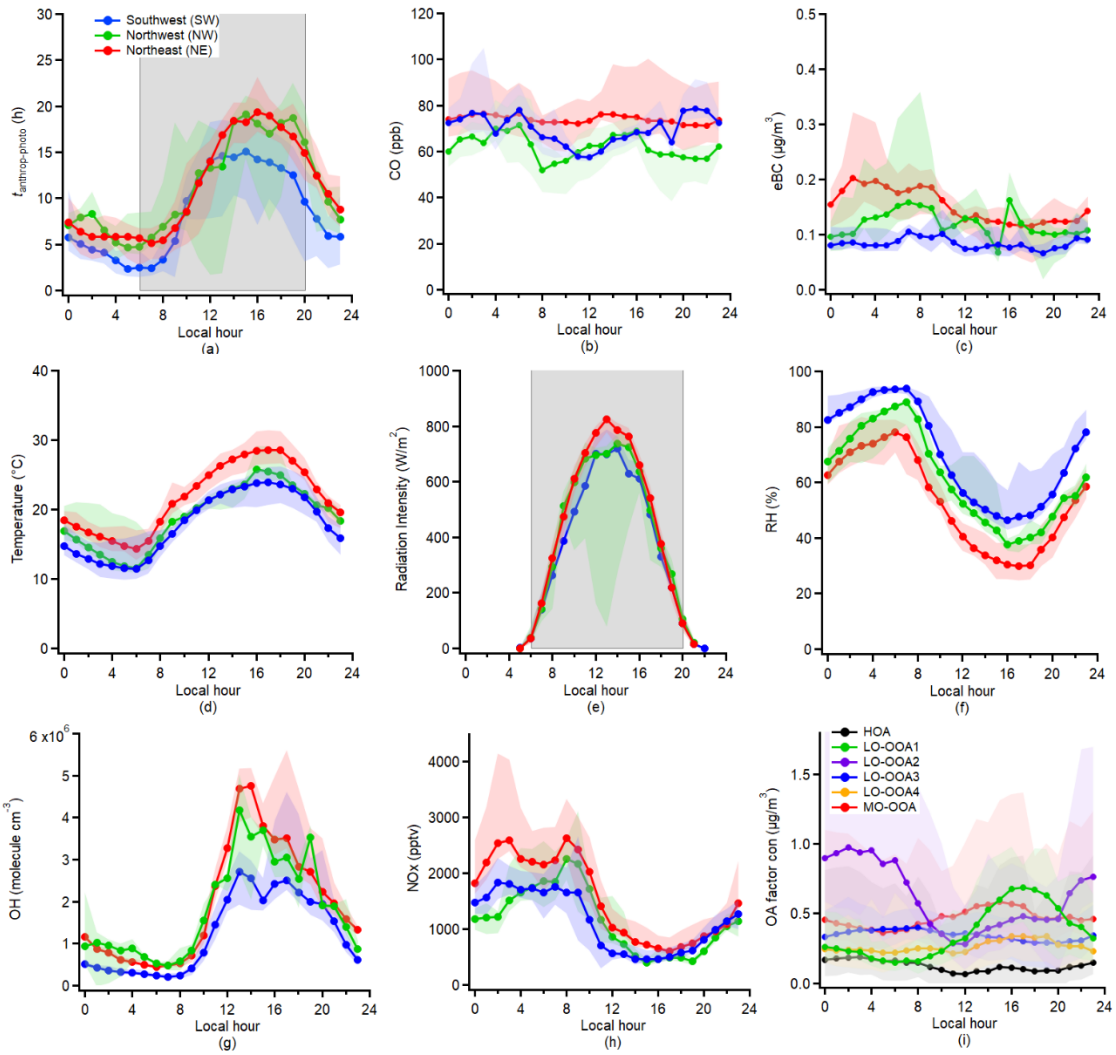

Figure 3: Diurnal variation of the (a) Relative anthropogenic photochemical age ($t_{anthrop-photo}$); (b) CO mixing ratio; (c) eBC mass concentration; (d) Temperature; (e) Radiation Intensity; (f) RH; (g) OH concentration; (h) NO_x concentration; (i) PMF-derived OA factors. The grey shades in (a) and (e) indicate the periods for the photochemical aging analysis. The lower and upper whiskers in the figure are the 25th and 75th percentiles, respectively.

Technical corrections:

1. Line 58: please add "Aerodyne" in front of the Aerosol Mass Spectrometer as there are more than one kind of aerosol mass spectrometer (e.g. AToFMS, PALMS) for its first appearance in your manuscript. The Aerodyne AMS/ACSM is just the most widely used commercial one.

Accept, we have corrected the term accordingly.

Source apportionment analysis on OA based on mass spectra from widely used instruments such as the Aerodyne Aerosol Mass Spectrometer (AMS) (Jayne et al., 2000) or Aerosol Chemical Speciation Monitor (ACSM) (Ng et al., 2011) can provide insight into its primary and secondary components.

2. Line 60-62: please specify your "Source apportionment analysis" is "Positive Matrix Factorization" because there are many ways of doing aerosol source apportionment, and the nomenclature of HOA, BBOA, COA etc is mostly for AMS-PMF analysis. You should add reference to Ulbrich et al. (2009) and Zhang et al., (2011) to this sentence for naming these OA factors.

Accept, we have revised the related descriptions.

The Positive Matrix Factorization (PMF) analysis of AMS/ACSM (Ulbrich et al., 2009; Zhang et al., 2011) derived POA typically includes hydrocarbon-like OA (HOA), biomass burning OA (BBOA), and cooking-related OA (COA), while the SOA (also referred as oxygenated OA (OOA), often used as a proxy for SOA) is often typically separated into Less-Oxidized OOA (LO-OOA) and More-Oxidized OOA (MO-OOA).

3. Line 68: please consider rephrasing to "..., an important part of OA primarily emitted or formed through the oxidation of VOCs in the presence…".

Accept, we have revised the related sentence:

Particulate organic nitrate (pON), an important component of OA primarily emitted or formed through the oxidation of VOCs oxidation in the presence of NO_x radicals and atmospheric oxidants, can substantially contribute to the total light-absorbing brown carbon (BrC) loadings

3. Figure 6(c) has one duplicated label (LO-OOA2).

Accept, we have corrected the typo here. We have also fixed the other typos following the comments from Reviewer #2.

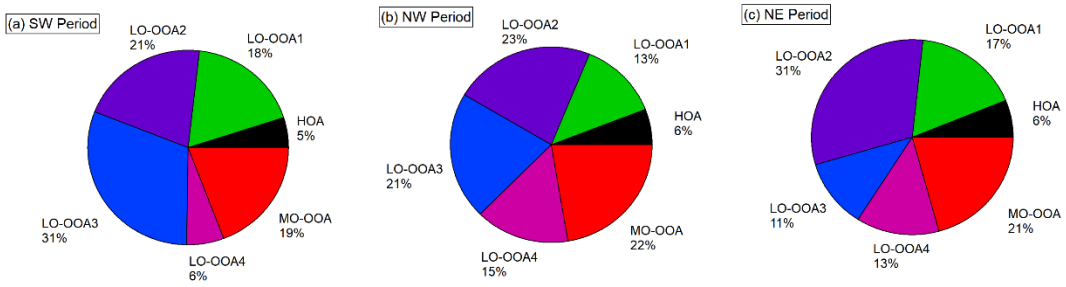

Figure 6: Pie charts for the mass fractions of different PMF-derived OA factors during the three different air mass dominated periods

Reviewer #2

This manuscript presents the impacts of the photochemical process on aerosol physicochemical and optical properties in a suburban forest near Paris. The authors characterize major PM1 components and gas-phase species, identify OA factors under different air mass origins, and investigate OOA evolution and their optical properties. The topic is relevant to ACP readers, and the idea of quantifying photochemical aging is interesting in principle. However, the current methodology has significant limitations, and some conclusions are not fully supported by the presented results, as detailed below. Therefore, I do not recommend the publication of this paper in ACP.

We appreciate the reviewer's acknowledgement of the scientific value of our work. To address the concerns raised, we have substantially revised the description of the methods. We have stated that the measurement was remote and the impact of fresh plumes was minor. The transported air mass was considered well mixed with anthropogenic emissions, therefore, we consider the NO_x/NO_y ratio a reasonable proxy for anthropogenic photochemical age and, by extension, for the air mass age at the site.

Major Comments

1. The key analysis relies on photochemical age, but I don't think it works for the sampling environment. The method works if one tracks the same air parcel from emission to downwind. But at this ground site, the air mass constantly changes. The method is heavily biased by the fresh plume close to the site. Many results may be confounded by the diurnal trend of calculated photochemical age. Why does isoprene concentration increase with photochemical age?

We appreciate the reviewer's concern. Firstly, we partly agree with the reviewer that the estimation of photochemical age based on NO_x/NO_y ratio did not address the biogenic emissions well. However, as the site is remote, we assume that air parcels from different regions were well mixed with anthropogenic (regional) and biogenic (regional and local) emissions. Secondly, the impact from the fresh plume close to the site during the daytime was minor. Indeed, the low CO and BC concentrations at the measurement site indicate that local anthropogenic emissions were very limited. We have also compared the below- and above-canopy results (presented in the revised supplementary) during the campaign to show that the local emissions had a negligible contribution to the results during the daytime.

To address the reviewer's concern, we determined that the relative photochemical age used in our study is a "Relative anthropogenic photochemical age" as it mainly captures the aging of anthropogenic pollutants in the mixed anthropogenic–biogenic air masses arriving at the site. We also discussed the uncertainty here that the "relative anthropogenic photochemical age" may slightly overestimate the photochemical age, and we have constrained "relative anthropogenic photochemical age" to 24 hours to avoid overestimation.

We have carefully revised and clarified these sections throughout the manuscript. We have revised the method Section 2.5 for photochemical aging estimation:

2.5 Relative anthropogenic photochemical age estimation

Photochemical processing of the mixed anthropogenic–biogenic air masses arriving at the measurement site was evaluated using the ratio between NO_x and NO_y as proposed by Kleinman et al. (2003); Kleinman et al. (2007), as done in previous ground-based measurement studies (Hayes et al., 2013; Ensberg et al., 2014). The relative anthropogenic photochemical age ($t_{\mathrm{anthrop-photo}}$) in this study is calculated following the method described by Nault et al. (2018):

$$t_{\mathrm{anthrop-photo}} = \frac{\ln\left(\frac{[NO_x]}{[NO_y]}\right)}{k_{OH+NO_2}[OH]_{avg}} \qquad (1)$$

Where $[NO_x]$ and $[NO_y]$ are the measured concentrations of NO_x and NO_y, respectively, $[OH]_{avg}$ is the average diurnal measured OH concentration during the campaign period, which was $1.6\ (\pm 1.3) \times 10^6$ molecules cm^{-3}. k_{OH+NO_2} is the rate coefficient of OH with NO_2 and is assumed to be

9.2×10^{-12} cm^3 $molecules^{-1}$ s^{-1} (Mollner et al., 2010). The estimated $t_{anthrop-photo}$ was constrained to the period of 6:00 – 20:00 European Summer Time (EST) according to the diurnal trend of the radiation intensity (presented in Figure 3(a) and 3(e)).

The results are expressed as "relative anthropogenic photochemical age" since the method mainly captures the aging of anthropogenic pollutants in the mixed anthropogenic–biogenic air masses arriving at the site. In addition, the potential short lifetime of NO_y in the forest (Andersen et al., 2024) may compromise the accuracy of absolute photochemical age calculation. Only the calculated $t_{anthrop-photo}$ within 1 day (24 hours) was used here to reduce the uncertainty of the estimated $t_{anthrop-photo}$ due to the potential short lifetime of HNO_3 and other oxidised reservoirs via deposition in the forest (Nguyen et al., 2015; Romer et al., 2016).

For reviewers query about the relationship between isoprene concentration and photochemical age, this was due to under daytime conditions, isoprene emissions were elevated. To avoid further misunderstood, we have revised the results and discussions here:

As shown in Figure 8(h), the ratio of isoprene to MVK+MACR decreased during the SW period, while its variation was limited during the NE period. This was likely due to both enhanced daytime isoprene emissions and more active photochemical process of MVK+MACR during the NE period.

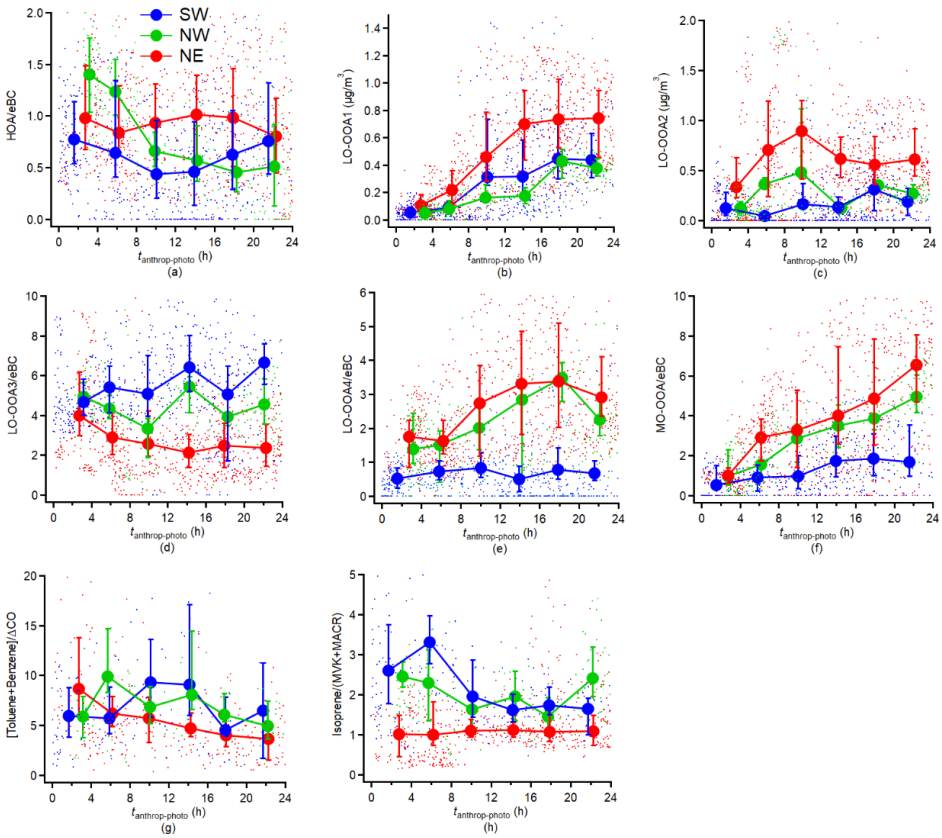

Figure 8: Variations in (a-f) HR-AMS PMF-derived OA factors; (g) Sum of Toluene and Benzene normalised concentration; (h) ratio between isoprene and MVK+MACR as a function of $t_{anthrop-photo}$. The results are averaged into four-hour intervals along $t_{anthrop-photo}$ and the error bar indicates the 25th and 75th percentiles, respectively.

2. OA is normalized to BC to account for dilution, but this approach only works if the species originates from the same source as BC. It may not be the case in this study. Line 220.

We accept the reviewer's comments. Given that the measurement site is a remote forested location, it is reasonable to assume that the air masses arriving there were enriched with anthropogenic primary carbonaceous aerosols and subsequently modified by secondary processes, the extent of which depends on their photochemical age. We have revised the related descriptions in our manuscript:

The air masses arriving at the measurement site were enriched with anthropogenic primary carbonaceous aerosols and subsequently modified by secondary processes. Concentrations of compounds presumed to be associated with anthropogenic sources were normalized by eBC to account for dilution, providing an indicator of secondary processing.

We have revised the Figure 8 to report the biogenic-related LO-OOA1 and LO-OOA2 in absolute terms, as this could overestimate their relative abundance. Please refer to our response to Major Comment 1 for the revised graph. We have also revised the discussions here:

The biogenic-related LO-OOA1 and LO-OOA2 were not normalized to eBC here. LO-OOA1 showed an increasing trend during all three periods. As shown in Figure 8(h), the ratio of isoprene to MVK+MACR decreased during the SW period, while its variation was limited during the NE period. This was likely due to both enhanced daytime isoprene emissions and more active photochemical process of MVK+MACR under the strong solar radiation and high temperatures characteristic of the NE period. All the periods illustrated a close relative production rate of around for LO-OOA1 which was 6.1 ($\pm$ 2.8) % h^{-1}, 8.7 ($\pm$ 3.6) % h^{-1} and 6.9 ($\pm$ 3.0) % h^{-1} for SW, NW, and NE period, respectively. However, LO-OOA2 showed no clear correlation with $t_{\mathrm{anthropo-photo}}$. As discussed in Section 3.2, LO-OOA2 can likely be attributed to SOA formation from locally emitted monoterpenes. As the Boundary Layer Height (BLH) increased during the daytime, LO-OOA2 was progressively diluted. Therefore, the variation of LO-OOA2 did not correspond to the evolution of $t_{\mathrm{anthropo-photo}}$.

3. Section 3.2 on source apportionment should be revised to make the conclusions convincing:

3.1 The correlation between OA factors and tracers is generally low. For example, the correlation between LO-OOA1 and isoprene is only 0.43. The comparison matrix in Fig. S9 should be moved to the main text.

We appreciate the reviewer's concern. In such a temperate forest, it's expected that the daytime BSOA factor to be strongly influenced by other precursors in addition to isoprene, as discussed in the main text. Conversely, LO-OOA2 has a correlation with monoterpenes of 0.79, which is quite high, particularly considering different atmospheric lifetimes of the gaseous species compared to the OA factor. The matrix has been relocated to the main text.

LO-OOA1 and LO-OOA2 exhibited very similar mass spectral profiles but distinct temporal patterns, with LO-OOA1 peaking during the daytime and LO-OOA2 during the nighttime. The correlation analysis indicates that they were associated with secondary formation from a mixture of biogenic precursors: while LO-OOA1 exhibited fair correlation with isoprene (r = 0.43), LO-OOA2 correlated more strongly with monoterpene (r = 0.79). The moderate correlation between LO-OOA1 and isoprene was to be expected in such a temperate forest, given the typical mixtures of BSOA precursors and the differing lifetimes of aerosol- and gas-phase compounds. Since monoterpenes emitted from local vegetation can form SOA through ozonolysis, OH- or NO_3- initiated reactions at night (Lee et al., 2016), this explains the nighttime peak of LO-OOA2. Good correlation (r = 0.63) was observed between LO-OOA3 and the sum of methyl vinyl ketone (MVK) and methacrolein (MACR), while a fair correlation (r = 0.45) was found between LO-OOA2 and MVK + MACR. Isoprene epoxydiols (IEPOX)-OOA was not identified through the HR-AMS results during the experiment period, as the mass spectral profiles of both LO-OOA1 and LO-OOA2 lacked the characteristic enhancement at m/z 82, a known tracer signal for IEPOX-OOA (Hu et al., 2015). However, both OOAs exhibited pronounced contributions at m/z 91.05, attributed to $C7H7^+$ fragments likely from thermal decomposition of dimers and oligomers on the vaporizer (Riva et al., 2016). These two biogenic-related LO-OOA factors contributed approximately 40% to 50% of the total OA mass concentration throughout the campaign period.

3.2 Be careful when correlating aerosol with gas species because they have different lifetimes.

We agree with review's comment. We have carefully revised our discussions regarding the correlations between short-lived isoprene and OOA factors accordingly. Please refer to our response to comment 3.1 for the revised context.

3.3 Line 274. The evidence to suggest marine emissions sources needs to be strengthened.

The interpretation of LO-OOA3 as a marine-influenced OOA factor is supported by two reasons: firstly, it is positive correlation with both RH and Chloride, secondly it is its prominence in back-trajectory clusters associated with oceanic influence. We were careful to the wording stating "suggest" for this factor may be influenced by the marine air mass here, as we agree that those links are circumstantial. In addition to direct marine emissions, we suggest another possibility that LO-OOA3 may form through aqueous-phase chemistry under high-RH conditions, particularly during periods dominated by marine air masses. Here is the revised text:

The diurnal trend shows that the LO-OOA3 concentration started increasing from the evening at around 8 pm and reached the peak in the early morning (between 6 and 8 am). The moderate positive correlation between LO-OOA3 and RH ($r = 0.45$) and Chl ($r = 0.4$) suggested that this OOA factor may be influenced by marine air masses. This interpretation is further supported by the larger mass fraction of LO-OOA3 observed during marine air mass-dominated periods (SW and NW periods) compared to continental periods (NE periods). However, no significant methanesulfonic acid (MSA) fragments were detected at m/z 79, 95, or 96. Consequently, the similarity between the LO-OOA3 mass spectral profile and the marine OOA factor previously reported in Paris was limited (Table S1). These results suggest that the marine influence at our site was dominated primarily by inorganic sea-salt Chl and its processed products, rather than by MSA-related organic aerosol. The highest N:C ratio among all the OOA factors for LO-OOA3 was observed suggesting that LO-OOA3 importantly contributed to the nitrogen-containing organics. However, the correlation between LO-OOA3 and pON was poor ($r = 0.06$). The mass spectral profile shows that the most abundant nitrogen-containing fragments were CHN^+ (m/z 27.01) and CH_4N^+ (m/z 30.03), which together contributed approximately 6% to the total LO-OOA3 signal. The presence of CH_4N^+ suggested that LO-OOA3 likely contained a contribution of reduced-N compounds such as organic amines (Ge et al., 2024). The LO-OOA3 likely originated from aqueous-phase chemistry under marine air mass dominance, where elevated RH (> 80%) at night-time promoted partitioning of nitrogen-containing organics into hygroscopic aerosol phases. Chen et al. (2019) also shows that the high RH condition promoted the formation of organic amines particles. At this suburban forest site, reduced nocturnal oxidant levels, especially during SW air mass periods, facilitated the accumulation of nitrogen-enriched LO-OOA3. In contrast, daytime photo-oxidation driven by OH radicals and secondary oxidants (e.g., O_3) effectively degraded LO-OOA3, as evidenced by strong inverse correlations between LO-OOA3 and photochemical-relate OVOCs (e.g. with MVK+MACR: $r = -0.69$).

3.4 Fig. S9 shows a stronger correlation between isoprene and MO-OOA ($r = 0.65$) than with LO-OOA1 ($r = 0.43$). Why is isoprene plotted only with LO-OOA1 in Fig. 4b?

We appreciate the reviewer's concern. While MO-OOA exhibited a stronger correlation, we considered that isoprene did not serve as a direct precursor tracer of MO-OOA due to its short lifetime. Instead, the observed correlation likely reflects photochemical control: under daytime conditions, isoprene emissions are elevated, and in parallel, oxidation of various precursors promotes MO-OOA formation. We have added the discussions here:

The MO-OOA was with the highest average O:C ratio (0.86) among all the factors, and dominant peaks were presented at m/z 28 (CO+) and 44 (CO2+). The good correlation between MO-OOA and isoprene was attributed to under daytime conditions, both elevated isoprene emissions and the oxidation of various

precursors leading to MO-OOA formation occurred simultaneously. The significant increase in MO-OOA observed during the afternoon, despite boundary layer dilution, indicates that summertime MO-OOA formation was strongly driven by active photochemical processes. Due to the reduction of photochemical activity during the SW period, the mass fraction of MO-OOA during the SW period was smaller than the fraction during the other periods. The wind rose analysis shows that the MO-OOA was contributed significantly from the anthropogenic polluted NE regions.

3.5 Line 265. The reported "good correlation" between LO-OOA and MVK+MACR should be quantified explicitly by providing the r value.

Accept, please refer to our response to comment 3.1 for the revised context. Please refer to our response to comment 3.1 for the revised context.

Minor Comments

1. In general, more contexts should be provided for clarity beyond referencing previous literature. For example:

1.1 Line 178. Describe more about the CIMS OH measurements.

Accept, we have added the related descriptions:

OH radicals were measured through the Chemical Ionisation Mass Spectrometry (CIMS, LPC2E), and more details about the instrument was described in (Kukui et al., 2008). Briefly, the CIMS determines OH radical concentrations by chemically converting sampled OH into H_2SO_4 by addition of SO_2 in a chemical conversion reactor in the presence of water vapour and oxygen (Eisele and Tanner, 1991). H_2SO_4 is detected by the mass spectrometer as HSO_4^- ion. To distinguish this signal from ambient H_2SO_4, the conversion process uses isotopically labelled $^{34}SO_4$ leading to the formation of $H_2^{34}SO_4$.

1.2 Line 103. Briefly describe the sampling site and its surroundings.

Accept, combine Reviewer #1's comment we have revised our related descriptions about the measurement site. Please refer to our reply to Reviewer #1's specific comment 3.6 for the revised context.

2. Line 115. Does the 0.1 L/min flow rate meet the cutoff specification for a PM2.5 cyclone, and would this low flow rate lead to potential sampling losses?

The whole sampling system has a total flow rate of 3 L min^{-1}, and 0.1 L min^{-1} is the HR-AMS flow rate. We have revised the related descriptions:

During the campaign, the HR-AMS conducted measurements with a flow rate of ~0.1 L min^{-1}, drawn from the main 3 L min^{-1} flow from a $PM_{2.5}$ cyclone and through a Nafion dryer.

3. Eqn 5 to calculate BrC. They didn't consider the lensing effect.

We appreciate the reviewer's concern. A Single Particle Soot Photometer (SP2, DMT) was only operational for a limited period during the campaign due to a technical issue, with data available partially between 11 July and 19 July. According to the SP2 results during its available periods, the mass ratio between the non-BC coating material and BC core material (MR) was 1.65 ($\pm$ 1.38) with density assumed as 1.8 g cm^{-3} for BC and 1.6 g cm^{-3} for non-BC coating, respectively. According to Liu et al. (2017), when MR is less than 3, the lensing effect becomes less pronounced, supporting the approximation of thinly coated BC particles as externally mixed in this study.

We have revised related sentences:

Then the σ_{abs} of BrC at 470 nm can be estimated as:

$$\boldsymbol{\sigma_{abs\ BrC,470} = \sigma_{abs,470} - \sigma_{abs\ BC,470}} \qquad (2)$$

A Single Particle Soot Photometer (SP2, DMT) was employed to characterise the BC mixing state but was only operational for a limited period during the campaign due to a technical issue, with data available partially between 11th July and 19th July. The coating thickness of BC particles was derived from the SP2 results using leading-edge only (LEO) method (Gao et al., 2007), and the mass ratio between the non-BC coating material and BC core material (MR) was 1.65 ($\pm$ 1.38), assuming densities as 1.8 g cm^{-3} for BC and 1.6 g cm^{-3} for non-BC coating. According to Liu et al. (2017), when MR is less than 3, the lensing effect becomes less pronounced. Therefore, the lensing effect of BC can be considered negligible in this study.

4. Line 330. It is strange that O:C does not increase. Further clarification is needed.

We appreciate the reviewer's concern. We considered that the OA observed at the measurement site was already relatively high when the estimated relative anthropogenic photochemical age is 0. As the photochemical processing progressed, the formation of additional LO-OOA could dilute the overall oxidation level, which also did not contribute to the increase of bulk O:C ratio. Previous study (Irei et al., 2015) also reported that the oxidation indicator did not increase with the increasing of photochemical age.

However, only during the NW period, there was a slight increase in the average bulk O:C ratio as a function of $t_{anthrop\text{-}photo}$. The average bulk O:C ratio did not show a corresponding increase with $t_{anthrop\text{-}photo}$ during the SW and NE period; instead, a slight decrease was observed at higher $t_{anthrop\text{-}photo}$ during the NE period. The relatively high O:C ratio at $t_{anthrop\text{-}photo}$ = 0 suggests that the observed regional background OA was already oxidised. With further photochemical processing, the evolution of O:C may become less significant, as reported in other field studies in remote station where oxidation indicators reached a steady state rather than continuing to rise with photochemical age (Irei et al., 2015). Furthermore, the decrease in O:C during the NE period was likely caused by the additional contribution of LO-OOA from photochemical processes, which diluted the overall oxidation level and lowered the average bulk O:C ratio.

5. Line 349. How to define the background CO?

The CO background was determined as the 5th percentile over the entire campaign period. Data influenced by biomass burning event were excluded from this analysis. We have included the related description in Section 3.4:

The background CO was defined as the 5th percentile of the entire campaign period (with BB influenced period removed) and was estimated to be 52 ppb.

6. Section 3.4. Cite Washenfelder et al., GRL, 2015.

Accept, we have revised the related discussions:

While LO-OOA1 and LO-OOA2 were predominantly associated with Biogenic SOA (BSOA) derived from isoprene and monoterpene oxidation, they typically displayed limited light absorption properties due to the prevalence of non-chromophoric oxygenated products (Flores et al., 2014; Laskin et al., 2015). This is consistent with a previous study in a suburban forest area in the US which also finds that BSOA was not correlated with the BrC absorption at short wavelengths (Washenfelder et al., 2015).

7. The manuscript uses coefficients from multiple linear regression to estimate MAC. A comparison between these estimated MAC values and directly measured MAC values from the literature should be included. The discussion should also address potential reasons for discrepancies across different factors. Additionally, interpreting correlation coefficients as contributions requires caution (i.e., variable standardization, multicollinearity, etc.). More statistical details should be provided to support this analysis.

We have revised our discussions.

We have included discussions to include the comparison between estimated MAC and measured MAC:

Table 1 presents the results of the regression factors of the MLR analysis between $\sigma_{\text{abs BrC,470}}$ and PMF-derived factors. The correlation coefficient is also presented to illustrate the contribution of each PMF-derived factor to the total BrC absorption during the whole experiment period. Interestingly, the LO-OOA3 and MO-OOA, which have the highest nitrogen content among all factors, also depict high MAC (regression coefficients). Nonetheless, their correlations with BrC differ markedly: LO-OOA3 displayed a significant negative partial correlation, whereas MO-OOA was strongly positively correlated. The HOA and LO-OOA4 also showed high MAC which were 0.47 m^2g^{-1} and 0.30 m^2g^{-1}, respectively, and they exhibited fair correlation with BrC. The MAC reported here was close to the results from other suburban areas. For example, Jiang et al. (2022) observed MAC values of 0.4 - 0.8 m^2g^{-1} at 375 nm for OA with O:C ratios between 0.4 and 0.6. In contrast, our MAC value was lower than the MAC observed near emission source. For example, Washenfelder et al. (2015) reported a MAC of 1.35 m^2g^{-1} at 365 nm for BB emitted OA. It is interesting to note that HOA, LO-OOA4 and MO-OOA also exhibited correlation with the pON, typically associated as an important component of BrC (Laskin et al., 2015)

We have calculated the Variance Inflation Factors (VIF) to support the correlation discussions. All VIF values were below 5, indicating that multicollinearity was not a concern. The partial correlation remained unchanged after variable standardization. We have revised the descriptions

The p-test ($p < 0.01$) was also applied to assess the statistical significance of each parameter. The MLR relationship between $\sigma_{\text{abs BrC,470}}$ and PMF-derived factors are formulated as:

$$\boldsymbol{\sigma_{\text{abs BrC,470}} = a_0 + \sum_i a_i [C_i]} \qquad (3)$$

Where a_0 represents the intercept, and a_i represents the regression coefficient for each PMF-derived factor C_i. These regression coefficients can be associated with the Mass Absorption Coefficients (MAC) of each PMF-derived factor. The Variance Inflation Factors (VIF) for all factors were below 5, indicating that multicollinearity was not a concern. The partial correlation remained unchanged after variable standardization.

We included the VIF results in the caption of Table 1.

Table 1. Results of multiple linear regression (MLR) between $\sigma_{abs\ BrC,470}$ and individual PMF-derived factors. The final regression excludes the LO-OOA1 due to its negative regression coefficient value (-0.06). The Variance Inflation Factors (VIF) for HOA, LO-OOA2, LO-OOA3, LO-OOA4, and MO-OOA were 1.48, 1.16, 1.71, 2.27 and 1.31, respectively. Results include all the PMF-derived OA factors that are presented in Table S2 in the supplementary.

Technical Corrections

1. A few typos were noted (e.g., "person correlation coefficient" in Line 248 and Fig. S9 caption; two "LO-OOA2" labels in Fig. 6a).

Accept, we have corrected the typo in our original manuscript. Line 248 has been revised as:

The Pearson correlation coefficient (r) between the HR-AMS PMF factors and the external tracers is presented in Figure S9 in the supplementary.

Figure S9 has been moved to the main text, and the revised content is presented in our response to Major comment 3.1. Revised Figure 6 has been presented in our response to Reviewer #1's Technical comment

2. The use of abbreviations is occasionally inconsistent. In some cases, terms are introduced without an abbreviation where one would be expected (e.g., aerosol mass spectrometer, Line 82), while in others the full term is unnecessarily repeated (e.g., the definition of PM1, Line 142).

Accept, we have revised Line 82 as:

Previous AMS studies (Stirnberg et al., 2021; Bressi et al., 2013; Petit et al., 2015; Healy et al., 2013) indicate that Paris is often affected by the mid-range to long-range transport pollutants attribute to the flat orography of the city.

Line 142 as:

The PM_1 aerosol optical absorption coefficient (units of $Mm^{-1} = 10^{-6}\ m^{-1}$) at seven different wavelengths (370, 470, 520, 590, 660, and 880 and 950 nm) was measured by a dual-spot aethalometer (AE33, Magee Sci.)

We have also revised the abbreviations used in other sections.

3. In Fig. 4a, please include labels to identify factors, such as HOA, LO-OOA1, etc., for improved readability.

Accept, we have revised Figure 4 as:

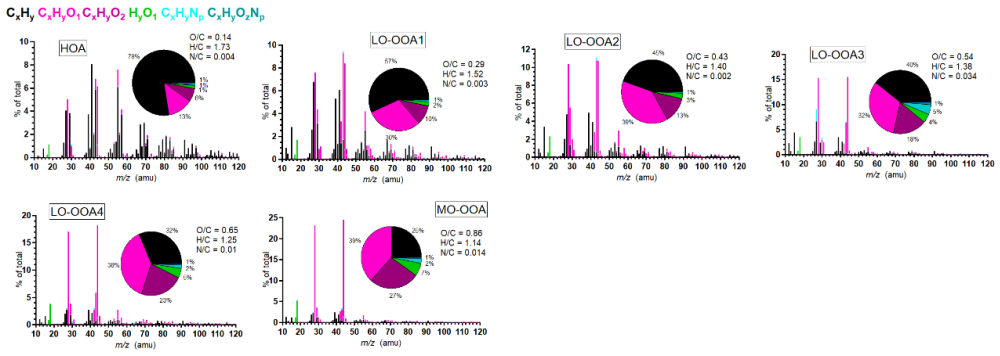

Figure 4: Average mass spectra for the PMF-derived OA factors.

Reference

Andersen, S. T., McGillen, M. R., Xue, C., Seubert, T., Dewald, P., Türk, G. N. T. E., Schuladen, J., Denjean, C., Etienne, J. C., Garrouste, O., Jamar, M., Harb, S., Cirtog, M., Michoud, V., Cazaunau, M., Bergé, A., Cantrell, C., Dusanter, S., Picquet-Varrault, B., Kukui, A., Mellouki, A., Carpenter, L. J., Lelieveld, J., and Crowley, J. N.: Measurement report: Sources, sinks, and lifetime of NOx in a suburban temperate forest at night, Atmos. Chem. Phys., 24, 11603–11618, 10.5194/acp-24-11603-2024, 2024.

Chen, Y., Tian, M., Huang, R. J., Shi, G., Wang, H., Peng, C., Cao, J., Wang, Q., Zhang, S., Guo, D., Zhang, L., and Yang, F.: Characterization of urban amine-containing particles in southwestern China: seasonal variation, source, and processing, Atmos. Chem. Phys., 19, 3245–3255, 10.5194/acp-19-3245-2019, 2019.

Crippa, M., El Haddad, I., Slowik, J. G., DeCarlo, P. F., Mohr, C., Heringa, M. F., Chirico, R., Marchand, N., Sciare, J., Baltensperger, U., and Prévôt, A. S. H.: Identification of marine and continental aerosol sources in Paris using high resolution aerosol mass spectrometry, Journal of Geophysical Research: Atmospheres, 118, 1950–1963, https://doi.org/10.1002/jgrd.50151, 2013.

DeCarlo, P. F., Kimmel, J. R., Trimborn, A., Northway, M. J., Jayne, J. T., Aiken, A. C., Gonin, M., Fuhrer, K., Horvath, T., Docherty, K. S., Worsnop, D. R., and Jimenez, J. L.: Field-Deployable, High-Resolution, Time-of-Flight Aerosol Mass Spectrometer, Analytical Chemistry, 78, 8281–8289, 10.1021/ac061249n, 2006.

Drugé, T., Nabat, P., Mallet, M., Michou, M., Rémy, S., and Dubovik, O.: Modeling radiative and climatic effects of brown carbon aerosols with the ARPEGE-Climat global climate model, Atmos. Chem. Phys., 22, 12167–12205, 10.5194/acp-22-12167-2022, 2022.

Eisele, F. L. and Tanner, D. J.: Ion-assisted tropospheric OH measurements, Journal of Geophysical Research: Atmospheres, 96, 9295–9308, https://doi.org/10.1029/91JD00198, 1991.

Ensberg, J. J., Hayes, P. L., Jimenez, J. L., Gilman, J. B., Kuster, W. C., de Gouw, J. A., Holloway, J. S., Gordon, T. D., Jathar, S., Robinson, A. L., and Seinfeld, J. H.: Emission factor ratios, SOA mass yields, and the impact of vehicular emissions on SOA formation, Atmospheric Chemistry and Physics, 14, 2383–2397, 10.5194/acp-14-2383-2014, 2014.

Franklin, E. B., Rossell, R. K., Vermeuel, M. P., De Groodt, A., Richard, K., Yee, L. D., Marcantonio, J., Maddaleno, T., Osburn, C., O'Brien, R. E., Commane, R., Mak, J. E., Goldstein, A. H., Millet, D. B., and Farmer, D. K.: Emerging drivers of urban aerosol increase global change vulnerability in a US megacity, npj Climate and Atmospheric Science, 8, 10.1038/s41612-025-01202-w, 2025.

Gao, R. S., Schwarz, J. P., Kelly, K. K., Fahey, D. W., Watts, L. A., Thompson, T. L., Spackman, J. R., Slowik, J. G., Cross, E. S., Han, J. H., Davidovits, P., Onasch, T. B., and Worsnop, D. R.: A Novel Method for Estimating Light-Scattering Properties of Soot Aerosols Using a Modified Single-Particle Soot Photometer, Aerosol Science and Technology, 41, 125–135, 10.1080/02786820601118398, 2007.

Ge, X., Sun, Y., Trousdell, J., Chen, M., and Zhang, Q.: Enhancing characterization of organic nitrogen components in aerosols and droplets using high-resolution aerosol mass spectrometry, Atmospheric Measurement Techniques, 17, 423–439, 10.5194/amt-17-423-2024, 2024.

Hayes, P. L., Ortega, A. M., Cubison, M. J., Froyd, K. D., Zhao, Y., Cliff, S. S., Hu, W. W., Toohey, D. W., Flynn, J. H., Lefer, B. L., Grossberg, N., Alvarez, S., Rappenglück, B., Taylor, J. W., Allan, J. D., Holloway, J. S., Gilman, J. B., Kuster, W. C., de Gouw, J. A., Massoli, P., Zhang, X., Liu, J., Weber, R. J., Corrigan, A. L., Russell, L. M., Isaacman, G., Worton, D. R., Kreisberg, N. M., Goldstein, A. H., Thalman, R., Waxman, E. M., Volkamer, R., Lin, Y. H., Surratt, J. D., Kleindienst, T. E., Offenberg, J. H., Dusanter, S., Griffith, S., Stevens, P. S., Brioude, J., Angevine, W. M., and Jimenez, J. L.: Organic aerosol composition and sources in Pasadena, California, during the 2010 CalNex campaign, Journal of Geophysical Research: Atmospheres, 118, 9233–9257, https://doi.org/10.1002/jgrd.50530, 2013.

Hu, W. W., Campuzano-Jost, P., Palm, B. B., Day, D. A., Ortega, A. M., Hayes, P. L., Krechmer, J. E., Chen, Q., Kuwata, M., Liu, Y. J., de Sá, S. S., McKinney, K., Martin, S. T., Hu, M., Budisulistiorini, S. H., Riva, M., Surratt, J. D., St. Clair, J. M., Isaacman-Van Wertz, G., Yee, L. D., Goldstein, A. H., Carbone, S., Brito, J., Artaxo, P., de Gouw, J. A., Koss, A., Wisthaler, A., Mikoviny, T., Karl, T., Kaser, L., Jud, W., Hansel, A., Docherty, K. S., Alexander, M. L., Robinson, N. H., Coe, H., Allan, J. D., Canagaratna, M. R., Paulot, F., and Jimenez, J. L.: Characterization of a real-time tracer for isoprene epoxydiols-derived secondary organic aerosol (IEPOX-SOA) from aerosol mass spectrometer measurements, Atmos. Chem. Phys., 15, 11807–11833, 10.5194/acp-15-11807-2015, 2015.

Irei, S., Takami, A., Sadanaga, Y., Miyoshi, T., Arakaki, T., Sato, K., Kaneyasu, N., Bandow, H., and Hatakeyama, S.: Transboundary secondary organic aerosol in western Japan: An observed limitation of the f44 oxidation indicator, Atmospheric Environment, 120, 71–75, https://doi.org/10.1016/j.atmosenv.2015.08.070, 2015.

Jeon, S., Walker, M. J., Sueper, D. T., Day, D. A., Handschy, A. V., Jimenez, J. L., and Williams, B. J.:

A searchable database and mass spectral comparison tool for the Aerosol Mass Spectrometer (AMS) and the Aerosol Chemical Speciation Monitor (ACSM), Atmos. Meas. Tech., 16, 6075–6095, 10.5194/amt-16-6075-2023, 2023.
Jiang, X., Liu, D., Li, Q., Tian, P., Wu, Y., Li, S., Hu, K., Ding, S., Bi, K., Li, R., Huang, M., Ding, D., Chen, Q., Kong, S., Li, W., Pang, Y., and He, D.: Connecting the Light Absorption of Atmospheric Organic Aerosols with Oxidation State and Polarity, Environmental Science & Technology, 56, 12873–12885, 10.1021/acs.est.2c02202, 2022.
Kleinman, L. I., Daum, P. H., Lee, Y. N., Nunnermacker, L. J., Springston, S. R., Weinstein-Lloyd, J., Hyde, P., Doskey, P., Rudolph, J., Fast, J., and Berkowitz, C.: Photochemical age determinations in the Phoenix metropolitan area, Journal of Geophysical Research: Atmospheres, 108, https://doi.org/10.1029/2002JD002621, 2003.
Kleinman, L. I., Daum, P. H., Lee, Y.-N., Senum, G. I., Springston, S. R., Wang, J., Berkowitz, C., Hubbe, J., Zaveri, R. A., Brechtel, F. J., Jayne, J., Onasch, T. B., and Worsnop, D.: Aircraft observations of aerosol composition and ageing in New England and Mid-Atlantic States during the summer 2002 New England Air Quality Study field campaign, Journal of Geophysical Research: Atmospheres, 112, https://doi.org/10.1029/2006JD007786, 2007.
Kukui, A., Ancellet, G., and Le Bras, G.: Chemical ionisation mass spectrometer for measurements of OH and Peroxy radical concentrations in moderately polluted atmospheres, Journal of Atmospheric Chemistry, 61, 133–154, 10.1007/s10874-009-9130-9, 2008.
Laskin, A., Laskin, J., and Nizkorodov, S. A.: Chemistry of Atmospheric Brown Carbon, Chemical Reviews, 115, 4335–4382, 10.1021/cr5006167, 2015.
Lee, A. K. Y., Abbatt, J. P. D., Leaitch, W. R., Li, S. M., Sjostedt, S. J., Wentzell, J. J. B., Liggio, J., and Macdonald, A. M.: Substantial secondary organic aerosol formation in a coniferous forest: observations of both day- and nighttime chemistry, Atmos. Chem. Phys., 16, 6721–6733, 10.5194/acp-16-6721-2016, 2016.
Liu, D., Whitehead, J., Alfarra, M. R., Reyes-Villegas, E., Spracklen, Dominick V., Reddington, Carly L., Kong, S., Williams, Paul I., Ting, Y.-C., Haslett, S., Taylor, Jonathan W., Flynn, Michael J., Morgan, William T., McFiggans, G., Coe, H., and Allan, James D.: Black-carbon absorption enhancement in the atmosphere determined by particle mixing state, Nature Geoscience, 10, 184–188, 10.1038/ngeo2901, 2017.
Middlebrook, A. M., Bahreini, R., Jimenez, J. L., and Canagaratna, M. R.: Evaluation of Composition-Dependent Collection Efficiencies for the Aerodyne Aerosol Mass Spectrometer using Field Data, Aerosol Science and Technology, 46, 258–271, 10.1080/02786826.2011.620041, 2012.
Mollner, A. K., Valluvadasan, S., Feng, L., Sprague, M. K., Okumura, M., Milligan, D. B., Bloss, W. J., Sander, S. P., Martien, P. T., Harley, R. A., McCoy, A. B., and Carter, W. P. L.: Rate of Gas Phase Association of Hydroxyl Radical and Nitrogen Dioxide, Science, 330, 646–649, 10.1126/science.1193030, 2010.
Nault, B. A., Campuzano-Jost, P., Day, D. A., Schroder, J. C., Anderson, B., Beyersdorf, A. J., Blake, D. R., Brune, W. H., Choi, Y., Corr, C. A., de Gouw, J. A., Dibb, J., DiGangi, J. P., Diskin, G. S., Fried, A., Huey, L. G., Kim, M. J., Knote, C. J., Lamb, K. D., Lee, T., Park, T., Pusede, S. E., Scheuer, E., Thornhill, K. L., Woo, J. H., and Jimenez, J. L.: Secondary organic aerosol production from local emissions dominates the organic aerosol budget over Seoul, South Korea, during KORUS-AQ, Atmos. Chem. Phys., 18, 17769–17800, 10.5194/acp-18-17769-2018, 2018.
Nguyen, T. B., Crounse, J. D., Teng, A. P., St. Clair, J. M., Paulot, F., Wolfe, G. M., and Wennberg, P. O.: Rapid deposition of oxidized biogenic compounds to a temperate forest, Proceedings of the National Academy of Sciences, 112, E392–E401, doi:10.1073/pnas.1418702112, 2015.
Papachristopoulou, K., Raptis, I.-P., Gkikas, A., Fountoulakis, I., Masoom, A., and Kazadzis, S.: Aerosol optical depth regime over megacities of the world, Atmospheric Chemistry and Physics, 22, 15703–15727, 10.5194/acp-22-15703-2022, 2022.
Riva, M., Budisulistiorini, S. H., Chen, Y., Zhang, Z., D'Ambro, E. L., Zhang, X., Gold, A., Turpin, B. J., Thornton, J. A., Canagaratna, M. R., and Surratt, J. D.: Chemical Characterization of Secondary Organic Aerosol from Oxidation of Isoprene Hydroxyhydroperoxides, Environmental Science & Technology, 50, 9889–9899, 10.1021/acs.est.6b02511, 2016.
Romer, P. S., Duffey, K. C., Wooldridge, P. J., Allen, H. M., Ayres, B. R., Brown, S. S., Brune, W. H., Crounse, J. D., de Gouw, J., Draper, D. C., Feiner, P. A., Fry, J. L., Goldstein, A. H., Koss, A., Misztal, P. K., Nguyen, T. B., Olson, K., Teng, A. P., Wennberg, P. O., Wild, R. J., Zhang, L., and Cohen, R. C.: The lifetime of nitrogen oxides in an isoprene-dominated forest, Atmos. Chem. Phys., 16, 7623–7637, 10.5194/acp-16-7623-2016, 2016.
Ulbrich, I. M., Canagaratna, M. R., Zhang, Q., Worsnop, D. R., and Jimenez, J. L.: Interpretation of organic components from Positive Matrix Factorization of aerosol mass spectrometric data, Atmos.

Chem. Phys., 9, 2891–2918, 10.5194/acp-9-2891-2009, 2009.
von der Weiden, S. L., Drewnick, F., and Borrmann, S.: Particle Loss Calculator – a new software tool for the assessment of the performance of aerosol inlet systems, Atmos. Meas. Tech., 2, 479–494, 10.5194/amt-2-479-2009, 2009.
Washenfelder, R. A., Attwood, A. R., Brock, C. A., Guo, H., Xu, L., Weber, R. J., Ng, N. L., Allen, H. M., Ayres, B. R., Baumann, K., Cohen, R. C., Draper, D. C., Duffey, K. C., Edgerton, E., Fry, J. L., Hu, W. W., Jimenez, J. L., Palm, B. B., Romer, P., Stone, E. A., Wooldridge, P. J., and Brown, S. S.: Biomass burning dominates brown carbon absorption in the rural southeastern United States, Geophysical Research Letters, 42, 653–664, https://doi.org/10.1002/2014GL062444, 2015.
Zhang, L., Wilson, J. P., MacDonald, B., Zhang, W., and Yu, T.: The changing PM2.5 dynamics of global megacities based on long-term remotely sensed observations, Environment International, 142, 105862, https://doi.org/10.1016/j.envint.2020.105862, 2020.
Zhang, Q., Jimenez, J. L., Canagaratna, M. R., Ulbrich, I. M., Ng, N. L., Worsnop, D. R., and Sun, Y.: Understanding atmospheric organic aerosols via factor analysis of aerosol mass spectrometry: a review, Analytical and Bioanalytical Chemistry, 401, 3045–3067, 10.1007/s00216-011-5355-y, 2011.